Unintentional Islanding Detection for Type-I Wind Turbine Generators Using Feeder Protection Relays: A Hardware-in-the-Loop Test

Srinivasa Rao Kamala, Jeewon Choi, Rachid Darbali-Zamora
Sandia National Laboratories, Albuquerque, New Mexico, USA

2024 56th North American Power Symposium (NAPS) | 979-8-3315-2103-5/24/$31.00 ©2024 IEEE | DOI: 10.1109/NAPS61145.2024.10741658

***Abstract*—Unintentional islanding (UI) detection is one of the primary concerns to be addressed in power systems with increasing windfarm penetration. For type-I wind turbine generators (WTGs) that lack advanced control capabilities, passive UI detection methods can be applied using external devices such as feeder protection relays. This paper presents an examination of UI detection for a type-I WTG using the commercial feeder protection relay SEL-751. The vector shift and the fast rate-of-change-of-frequency (ROCOF) elements supported by the SEL-751 for islanding detection were tested under various loading conditions in a hardware-in-the-loop (HIL) testbed using OPAL-RT simulator.**

***Index Terms*—Unintentional islanding detection, type-I wind turbine generator, vector shift detection, fast rate-of-change-of-frequency protection.**

I. Introduction

Unintentional islanding (UI) detection is crucial for the reliable and stable operation of a power system, particularly in the areas where wind turbine systems are widely deployed. Wind farms and turbines are designed to remain connected to the grid and are not permitted to disconnect in the event of a disturbance or failure [2]. Islanding is not always unintentional in and of itself, but inaccurate UI can have negative consequences for customer and utility equipment integrity. Even if the UI period is short, system stability remains a concern. As a result, the UI detection is one of the major issues which has been taken into account in national grid codes and international standards.

Passive and active UI detections are two important methodologies available in the literature [4]. The passive detection approach monitors the electrical parameters at the point of common coupling (PCC), mainly voltage and frequency, and compares them to predetermined threshold levels. If the measured parameters at the PCC are above the threshold, islanding is detected [4]. Active methods inject disturbances into the system to detects the islanding based on system responses via the measured signals locally and usually these methods requires a power electronic converters [4].

According to IEEE 1547.1 [3] standard, a generator should detect an UI condition and cease to energize within 2 s. Because type I and II wind turbines lack an internal power converter, passive UI detection methods can be used, and protective relays are commonly used for UI protection in passive methods. The main objectives of this study are to validate the Siva type-I WTG field data collected from the installation site and assessing the capability of the SEL-751 feeder protection relay for UI detection in a system with type-I WTG connected to the grid. To this end, this paper presents the following contributions: 1) A MATLAB/Simulink model of a commercially available type-I WTG, Siva 250/50, is developed and is validated with field data, 2) A hardware-in-the-loop (HIL) testbed to evaluate the UI detection functionality of a commercial feeder protection relay SEL-751 is implemented, 3) The performance of SEL-751 under various islanding scenarios are tested and the results are provided.

The remainder of the paper is organized as follows: Section II discusses the Siva type-I WTG technical details, it's operation and control, field data validation in simulation model. Section III explains the SEL-751 relay's UI detection capability, using vector shift element 78VS and the rate of change of frequency element 81RF. Section IV presents experimental results for UI detection of relay in control hardware-in-loop under different loading conditions. Section V concludes the paper.

II. Type-I WTG Model Development

Siva 250/50 is a type-I WTG with a rotor diameter of 30 m and a nominal power of 250 kW [5]. The generator is a dual-wound, 6/8 pole squirrel cage asynchronous generator. In periods with low wind speeds the generator operates on the 8 pole, 50 kW stator winding and at higher wind speeds generator operates on the 6 pole, 250 kW stator winding. The

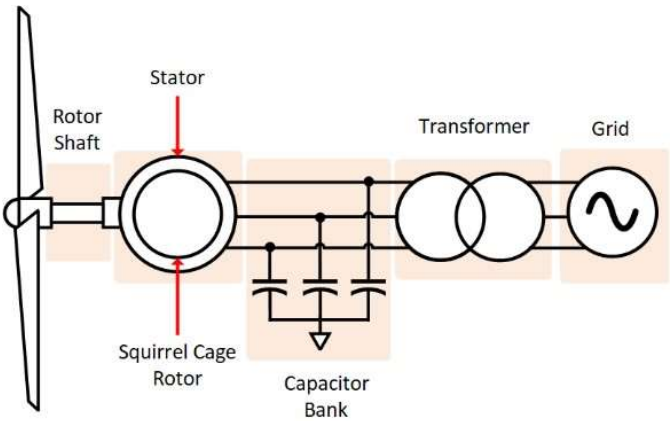

Fig. 1. Diagram of a type-I WTG connected to the grid [1].

Authorized licensed use limited to: Sandia National Laboratories. Downloaded on November 05,2025 at 19:49:17 UTC from IEEE Xplore. Restrictions apply.

generator operates at 480V, 60 Hz, and has a synchronous speed of 1200 RPM/900 RPM which corresponds to 6/8 poles. The typical block diagram of the type-I WTG is shown in Fig. 1. The technical specifications of the WTG are summarized in Table I.

TABLE I
TECHNICAL SPECIFICATIONS OF SIVA 250/50

	Rating	Unit
Start-up wind speed	3-4	m/s
Cutout wind speed	25	m/s
Speed at nominal output	14	m/s
Generator type	dual wound, asynchronous	-
Generator poles	6/8	-
Synchronous speed	1200/900	RPM
Nominal power	250/50	kW
Nominal voltage	480	V
Nominal frequency	60	Hz

A. Operation and Control of Siva 250/50

Siva 250/50 uses the MITA-Teknik controller [6] for its operation at various wind speeds. The MITA-Teknik controller has several control features, including grid-connection control, isolated mode control, switching between two rotor windings, fault ride through (FRT), and yaw motor control etc. In grid-connection mode, Siva 250/50 is regulated by the MITA-Teknik controller at various wind speeds as follows:

- If the wind speed exceeds 5.5 m/s, the WTG with rotor 2 (6 pole, 1200 RPM, 250 kW) connects to the grid and feeds power.
- The WTG with rotor 1 (8 pole, 900 RPM, 50 kW) connects to the grid and feeds power when wind speed is less than 5.5 m/s and greater than 3.5 m/s.
- If the wind speed is less than 3.5 m/s and greater than 2 m/s, the WTG acts as a induction motor and draws power from grid.
- If the wind speed drops below 2 m/s, the WTG disconnects from the grid.

B. Model validation

Siva 250/50 is modeled using MATLAB/Simulink simulation environment. The model is validated with the field data collected for the grid-connected mode of operation at various wind speeds from the installation site in Buffalo, New York [5]. The voltage, frequency, rotor speed, and active power output of the model simulation at various wind speeds are compared to the field data in Fig. 2. It can be observed from Fig. 2a and Fig. 2b that, voltage and frequency of the WTG is equal to 277 V and 60 Hz, respectively, at various wind speeds. The implementation of the rotor winding switching control of MITA-Teknik is also validated in Fig. 2c. The WTG speed is below 900 RPM for wind speeds 2-3.5 m/s, at 900 RPM for wind speeds 3.5-5.5 m/s and at 1200 RPM for wind speed above 5.5 m/s. Notice from these results that the WTG active power changes accordingly, as shown in Fig. 2d.

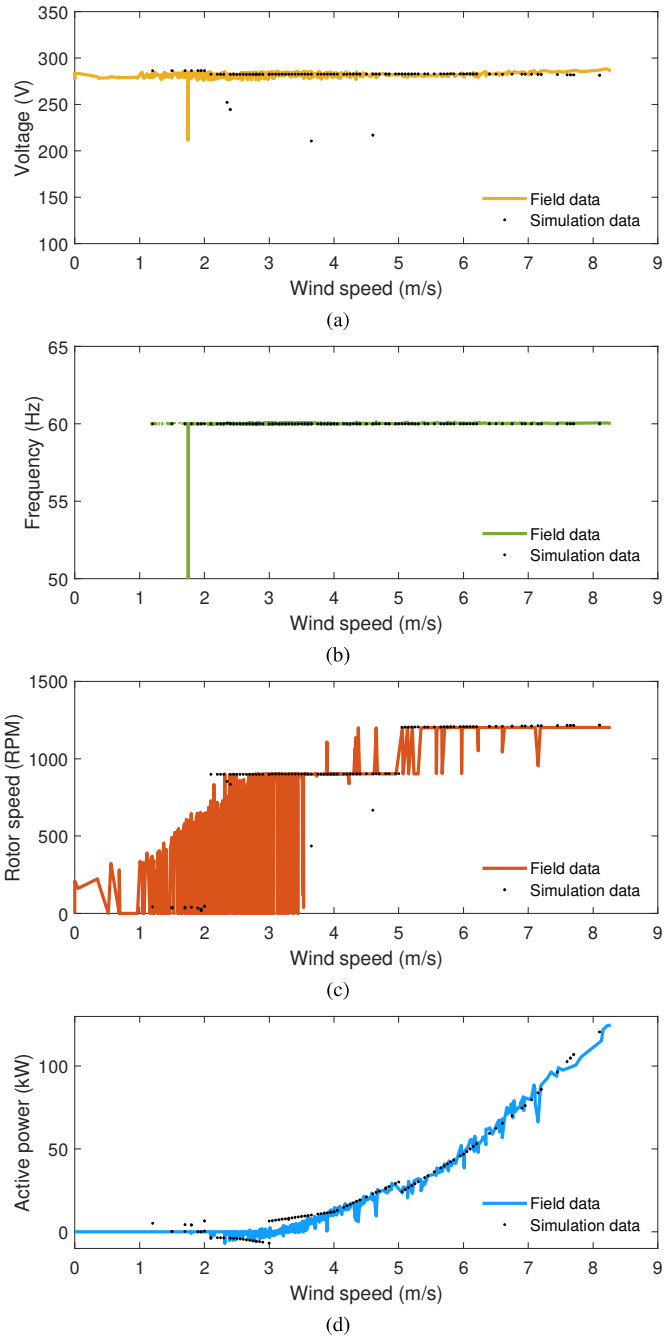

Fig. 2. WTG model is validated with the field data: (a) Voltage; (b) Frequency; (c) Rotor speed; (d) Active power.

III. UI DETECTION USING FEEDER PROTECTION RELAY

For the type-I WTG, an external protection device may be necessary to enable islanding detection. The commercially available feeder protection relay SEL-751 includes several islanding detection elements and can be utilized in combination with the type-I WTG. This subsections summarize the vector shift element and the fast rate-of-change-of-frequency (ROCOF) feature supported by the SEL-751 for islanding detection.

Authorized licensed use limited to: Sandia National Laboratories. Downloaded on November 05,2025 at 19:49:17 UTC from IEEE Xplore. Restrictions apply.

A. Vector shift element (78VS)

The control logic diagram of the 78VS vector shift element of the SEL-751 relay is shown in Fig. 3. Zero-crossing detection logic is used to perform the period calculations on each of the voltage inputs VA, VB and VC. The angle shift calculation element block calculates the difference between the present period on each phase with the corresponding reference period in each quarter-cycle. This difference is expressed in degrees to determine the angle shift and compares it against the angle shift threshold setting 78VSAPU. The count calculator receives angle shift detection information from all three phases and records the number of times that the angle shift threshold of all phases has been exceeded in two consecutive quarter-cycles. The output of the count calculator is asserted if the count exceeds four.

The short circuit conditions can also induce the voltage angle shift. In order to prevent false tripping from the short circuit conditions, the vector shift element is blocked for undervoltage conditions. If any phase voltage drops below the voltage supervision threshold setting 78VS59, the output of the vector shift element will be blocked. VNOM is the nominal RMS phase to phase voltage of the system. If both the angle shift counter and voltage supervision are satisfied and no other blocking conditions exist, the output 78VSO is asserted.The settings for the 78VS element are given in Table II. E78VS is the enable variable for the 78VS.

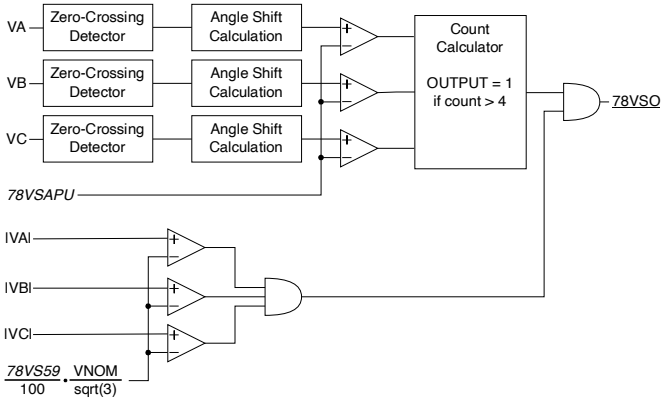

Fig. 3. Logic diagram of the 78VS vector shift element. Variables in italic are the settings and the underlined variable is the output.

TABLE II
78VS VECTOR SHIFT ELEMENT SETTINGS

Setting name	Setting range	Value	Unit
E78VS	Y, N	Y	-
78VSAPU	2.0 - 30.0	2.0	deg
78VS59	20.0 - 100.0	80	%

B. Fast ROCOF protection (81RF)

The fast ROCOF element, 81RF, complements the 78VS vector shift element by providing more dependable protection due to its fast response to ROCOF. The logic diagram of the 81RF element is shown in Fig. 4 [7]. The 81RF element uses a characteristic based on frequency deviation from nominal frequency (DF) and ROCOF (DF3C) to detect islanding conditions. DF3C is the ROCOF calculated over a 3-cycle window. The characteristics can be configured by the settings 81RFRP and 81RFDFP, which are the frequency difference setpoint and the ROCOF setpoint. The settings 81RFPU and 81RFDP are the pickup and dropout delays for 81RF. 81RFT is the output of the 81RF element and returns 1 when asserted. The settings required for the 81RF element are given in Table III. E81RF is the enable variable for the 81RF.

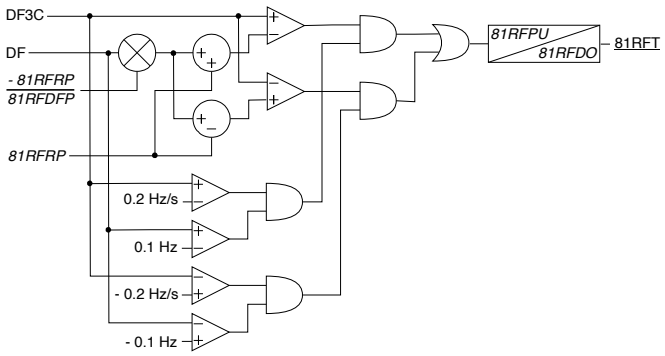

Fig. 4. Logic diagram of the 81RF fast ROCOF element. Variables in italic are the settings and the underlined variable is the output.

TABLE III
81RF FAST ROCOF SETTINGS

Setting name	Setting range	Value	Unit
E81RF	Y, N	Y	-
81RFDFP	0.1 - 10.0	1.0	Hz
81RFRP	0.2 - 15.0	2.5	Hz/s
81RFPU	0.10 - 1.00	0.10	s
81RFDO	0.00 - 1.00	0.10	s

IV. EXPERIMENTAL RESULTS

In this section, the UI detection for type-I WTG using the SEL-751 is tested in the HIL testbed. Detecting UI events can be challenging under certain loading conditions. Most UI detection methods exhibit a non-detection zone (NDZ), where they fail to detect UI events when the load and generation are closely balanced. To address this challenge, UI events are simulated under different loading conditions: 1) overloaded, 2) balanced, and 3) underloaded. The test system used for the experiment, which includes a type-I WTG connected to the grid, is shown in Fig. 5. An UI event is simulated by opening the grid side circuit breaker CB1.

Authorized licensed use limited to: Sandia National Laboratories. Downloaded on November 05,2025 at 19:49:17 UTC from IEEE Xplore. Restrictions apply.

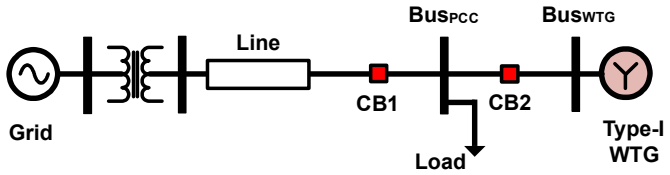

Fig. 5. Test system diagram implemented in MATLAB/Simulink: Type-I WTG connected to the main grid.

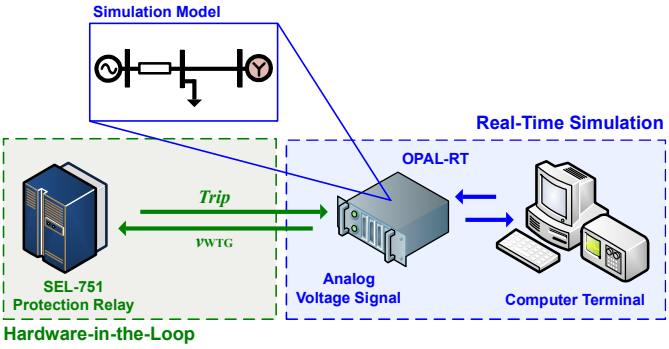

Fig. 6. HIL testbed for testing the SEL-751 using OPAL-RT. The voltage at the PCC is fed into the relay from the OPAL-RT analog board, and the trip signal from the relay is sent to the circuit breaker via GOOSE communication.

The HIL testbed is implemented using the OPAL-RT real-time simulator, as shown in Fig. 6. The test system in Fig. 5 is simulated in the OPAL-RT real-time simulator through the RT-LAB interface. The three phase voltages at the WTG bus are generated as analog signals through the OPAL-RT board and are fed to the SEL-751. The SEL-751 processes the voltage input and generates a trip signal based on the user defined trip function. The relay trip signal is subsequently sent to the WTG side circuit breaker CB2 in the real-time simulation environment via the Generic Object Oriented Substation Event (GOOSE) communication protocol.

A. Case 1: Overloaded condition

The grid side circuit breaker CB1 opens at 30 seconds, In this case, the load is 105% of the WTG output power and grid side breaker is opened at 30 seconds with wind speed is kept constant at 10 m/s. Fig. 7 (a) to (d) depicts the voltage, frequency of the WTG, phase angle and trip signals of the SEL-751 relay. Initially, the relay's 78VS element is deactivated, and the corresponding WTG voltage is shown in Fig. 7 (a) with blue line. In this scenario, the relay doesn't trip and the voltage drops with time and destabilizes the system. Next, the 78VS element is activated under the same loading condition and the relay trips at 30.85 s based on the phase angle thresh hold settings as illustrated in Fig. 7 (a) with red dotted line. The phase angles of three-phase voltages are shown in Fig. 7 (c) and the corresponding tripping signal 78VSO are shown in Fig. 7 (d), respectively.

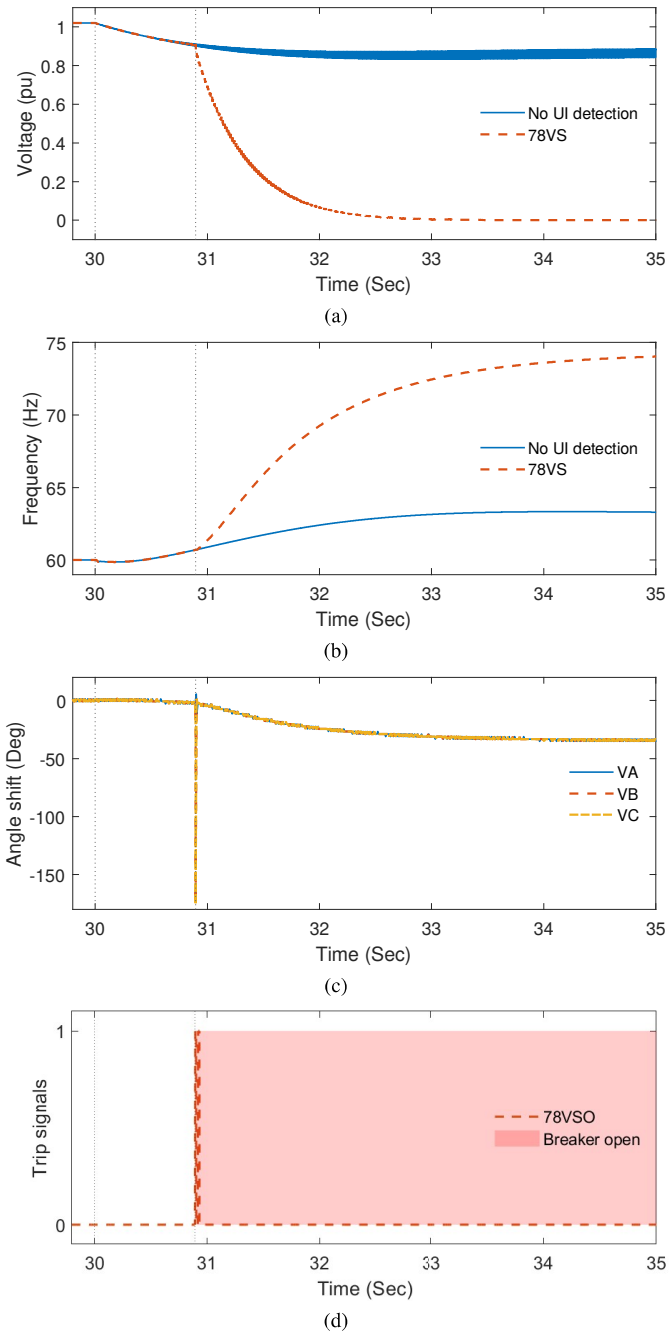

Fig. 7. UI detection using 78VS in Case 1: (a) Voltage; (b) Frequency; (c) Angle shift; (d) Trip signals.

B. Case 2: Load-generation balanced condition

In this case the load is 100% of the WTG power and the grid side breaker is opened at 30 s. Initially, the relay's 78VS element is activated and the corresponding WTG voltage is shown in Fig. 8 (a) (red line). In this scenario, the SEL-751 relay doesn't trip due to the phase shift not being above 2^o. Next, the 81RF element is also activated and the relay trips at 31.65 s based on the ROCOF settings, as shown in Fig. 7 (c) (purple dotted line). Fig. 8 (c) shows the SEL-751 relay

Authorized licensed use limited to: Sandia National Laboratories. Downloaded on November 05,2025 at 19:49:17 UTC from IEEE Xplore. Restrictions apply.

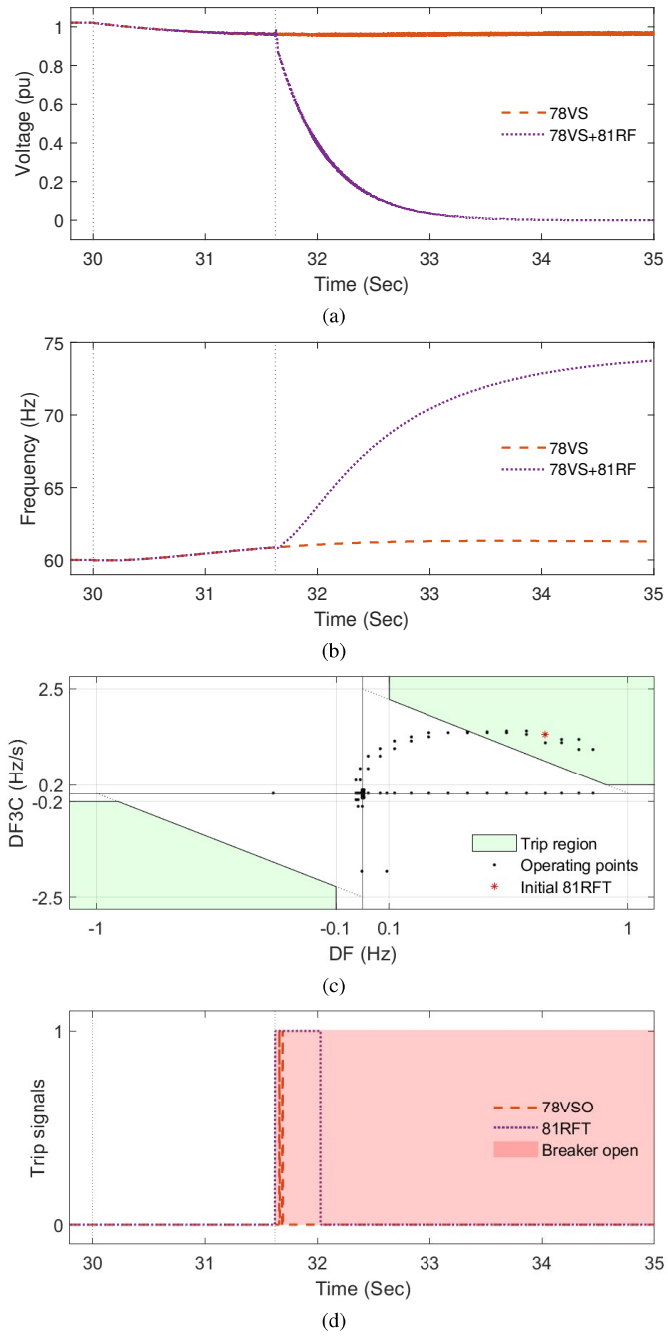

Fig. 8. UI detection using 78VS and 81RF in Case 2: (a) Voltage; (b) Frequency; (c) 81RF characteristics; (d) Trip signals.

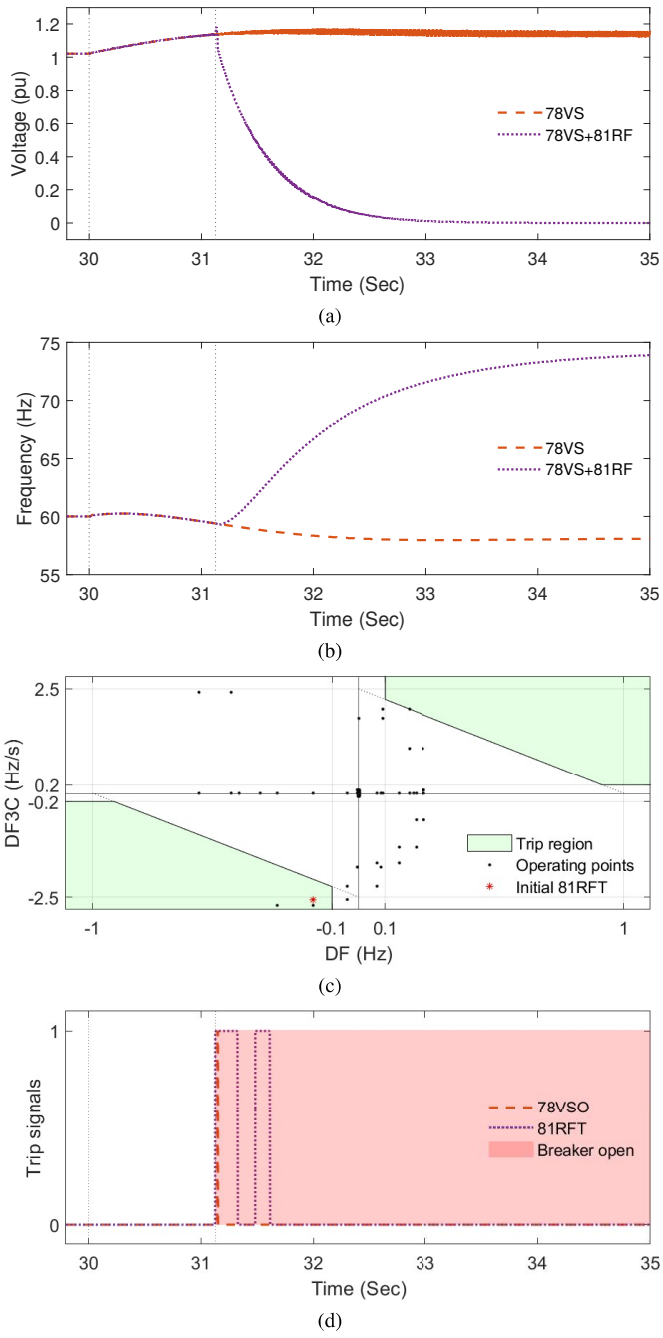

Fig. 9. UI detection using 78VS and 81RF in Case 3: (a) Voltage; (b) Frequency; (c) 81RF characteristics; (d) Trip signals.

trip region difference in frequency (DF) and rate of change in frequency (DF3C). Fig. 8 (d) shows the relay element 81RF response and trip signal 78VSO.

C. Case 3: Underloaded condition

In this case the load is 90% of the WTG out power with a fixed wind speed and grid side breaker is opened at 30 s. Initially, the relay's 78VS element is activated and the corresponding WTG voltage is shown in Fig. 9 (a) with red line. In this scenario, the SEL-751 relay doesn't trip because the phase shift is not above 2^o. Next, the 81RF element is also activated and the relay trips at 31.15 s based on the ROCOF settings as shown in Fig. 9 (c) with purple dotted line. Fig. 9 (c) depicts the SEL-751 relay trip region and Fig. 9 (d) shows the relay element 81RF response and trip signal 78VSO respectively. In Case II and Case III, 81RF element of relay responds faster than 78VS. In summary, in all the three critical loading conditions, SEL 751 relay is able to detect the UI condition based on VS and ROCOF in voltage.

Authorized licensed use limited to: Sandia National Laboratories. Downloaded on November 05,2025 at 19:49:17 UTC from IEEE Xplore. Restrictions apply.

V. Conclusions

This paper presents an examination of UI detection for a type-I WTG using the commercial feeder protection relay SEL-751. A MATLAB/Simulink model for the commercial type-I WTG Siva 250/50 was developed and verified with field data acquired from the installation site in Buffalo, New York. The test system, including the type-I WTG model connected to the grid, was simulated in real-time using OPAL-RT. The voltage at the WTG terminal was fed to the SEL-751, and the relay trip signal was sent to the circuit breaker in the test system model via the GOOSE protocol. The 78VS vector shift and 81RF fast ROCOF elements supported by the SEL-751 for UI detection were tested under three different load conditions: overloaded, balanced, and underloaded. In all three scenarios, the 78VS or 81RF elements detected the islanding event and isolated the WTG from the grid within 2 seconds.

Acknowledgement

This article has been authored by an employee of National Technology and Engineering Solutions of Sandia, LLC under Contract No. DE-NA0003525 with the U.S. Department of Energy (DOE). The employee owns all right, title and interest in and to the article and is solely responsible for its contents. The U.S. Government retains and the publisher, by accepting the article for publication, acknowledges that the U.S. Government retains a non-exclusive, paid up, irrevocable, worldwide license to publish or reproduce the published form of this article or allow others to do so, for U.S. Government purposes. The DOE will provide public access to these results of federally sponsored research in accordance with the DOE Public Access Plan.

The authors acknowledge the financial support provided by the U.S. DOE, Office of Energy Efficiency (EERE), Wind Energy Technology Office (WETO) for the Wind Hybrid Integration Platform (WHIP) project under Work Breakdown Structure No. 1.2.6.701 as well as the contributions from Bret Barker, Patrick Gilman, Padma Kasthurirangan, Varun Kumar, Matthew J. Reno, and Adam K. Summers.

References

[1] Bianchi, Fernando D., Hernan De Battista, and Ricardo J. Mantz. "Wind turbine control systems: principles, modelling and gain scheduling design". Vol. 19. London: Springer, 2007.

[2] Honrubia-Escribano, A., et al. "Generic dynamic wind turbine models for power system stability analysis: A comprehensive review." *Renewable and Sustainable Energy Reviews 81 (2018)*: 1939-1952.

[3] "IEEE Application Guide for IEEE Std 1547(TM), IEEE Standard for Interconnecting Distributed Resources with Electric Power Systems," in *IEEE Std 1547.2-2008*, vol., no., pp.1-217, 15 April 2009.

[4] K. Naraghipour, K. Ahmed and C. Booth, "A Comprehensive Review of Islanding Detection Methods for Distribution Systems," 2020 9th International Conference on Renewable Energy Research and Application (ICRERA), Glasgow, UK, 2020, pp. 428-433

[5] https://buffalorenewables.green/distributed-wind/

[6] https://www.mita-teknik.com/

[7] https://selinc.com/products/751/

[8] E. Desarden-Carrero et al., "Evaluation of the IEEE Std 1547.1-2020 Unintentional Islanding Test Using Power Hardware-in-the-Loop",47th IEEE Photovoltaic Specialists Conference (PVSC), 2020, pp. 2262-2269.

Authorized licensed use limited to: Sandia National Laboratories. Downloaded on November 05,2025 at 19:49:17 UTC from IEEE Xplore. Restrictions apply.